AIAA JOURNAL
Vol. 44, No. 11, November 2006

Technical Notes

TECHNICAL NOTES are short manuscripts describing new developments or important results of a preliminary nature. These Notes should not exceed 2500 words (where a figure or table counts as 200 words). Following informal review by the Editors, they may be published within a few months of the date of receipt. Style requirements are the same as for regular contributions (see inside back cover).

Mean Velocity of Fully Developed Turbulent Pipe Flows

Zvi Rusak and James Meyerholz
Rensselaer Polytechnic Institute, Troy, New York 12180-3590

DOI: 10.2514/1.15054

Introduction

The mean flow profile of a turbulent flow in a smooth channel or a pipe is a classical topic in fluid mechanics [1–4]. For fully developed turbulent pipe flows, von Kármán and Prandtl's pioneering analyses indicate two dominant regions: the near-wall laminar sublayer and the turbulent region away from the wall. The two regions are connected by a small intermediate buffer zone. In both regions, u^+, the mean velocity scaled with the friction speed u_τ, is a function of y^+, the distance from the wall scaled with the ratio of kinematic viscosity to friction speed ν/u_τ. This relationship $u^+ = f(y^+)$ is known as the classical "law-of-the-wall."

The Reynolds-averaged Navier–Stokes equation describes the mean axial speed of a fully developed turbulent flow and involves the viscous stresses and the turbulent Reynolds stresses. This equation is unclosed because there is no physical rule relating between the turbulent stresses and the mean axial speed. Yet, experiments show that the magnitudes of the stresses differ vastly for each region. Very near the wall, in the viscous sublayer where $y^+ < 5$, the Reynolds stress is negligible and u^+ grows linearly with y^+. Conversely, in the limit of an infinite Reynolds number, the turbulent inertial region where $y^+ > 70$ is characterized by a negligible viscous stress and a dominant Reynolds stress. Modeling the Reynolds stress in this region by the linear mixing-length approach of Prandtl [3] results in the "logarithmic velocity distribution law." The logarithmic relationship was also derived from a dimensional analysis requiring the continuity of the velocity gradient in the buffer zone when the Reynolds number is sufficiently high and using u_τ as the speed scale in both the near-wall and turbulent region [4]. In the buffer zone, the Reynolds and viscous stresses are of the same magnitude. Von Kármán suggested that in the buffer zone u^+ is also related to the logarithm of y^+. In both the buffer and turbulent zones, the logarithmic functions include two constants that may be determined experimentally. This semi-empirical approach showed a nice agreement with measurements [2]. It also resulted in "Prandtl's universal law of friction for smooth pipes" which relates between the friction factor and the Reynolds number and agrees with data. Note that van Driest [5] proposed a damping function for the turbulent stress in the viscous sublayer and the buffer zone which resulted in a good prediction of the mean velocity in these regions.

In recent years, new approaches raised controversy about the scales of both distance and speed in the outer or core region for pipe flows. The pipe radius has been proposed as an additional dominant length scale. Arguments have been made for the velocity scale to be either the maximum (centerline) speed [6] or the velocity deficit [7]. The functional form of the scaling law in the overlap region is a subject of even greater controversy. It has been suggested that a power law rather than a log law governs the relationship between velocity and distance from the wall [6–8]. Note, however, that Wosnik et al. [6], Zagarola and Smits [7], and Barenblatt [8] power laws are derived from different approaches. For a thorough review of the scales in turbulent pipe flows, see Pope [9].

Wosnik et al. [6] proposed a more detailed description of the pipe flow structure, see also Pope, [9] chapter 7. They divided the flow into the main "viscous sublayer," "overlap," and "outer" regions. The near-wall region, where $0 < y^+ < 30$, is composed of the linear viscous sublayer and the buffer zone. The overlap region, where $30 < y^+ < 0.1K$ and K is the Kármán number, is built of a mesolayer and the inertial sublayer. The viscous sublayer and overlap region constitute the inner region. The outer region extends from $0.1K$ to the pipe centerline. The similarity structures of the flow in the inner and outer regions at a finite Reynolds number were analyzed based on the Reynolds-averaged boundary-layer equation. It was found through the matching of the inner and outer velocity profiles and their derivatives that the flow in the overlap region (specifically in the mesolayer) may be described by a power law. A composite velocity profile for the entire range of the boundary layer was proposed. George and Castillo [10] and Wosnik et al. [6] also emphasized the universality of the velocity deficit profile in terms of the global distance y/δ or y/R in the outer region and its dependence on the Reynolds number in the inner region. They demonstrated the universality of the velocity profile $u^+ = f(y^+)$ in the inner region and its dependence on the Reynolds number in the outer region.

Zagarola and Smits [7] conducted careful experiments of turbulent flows in a pipe in Princeton's superpipe experimental apparatus. Using compressed (pressurized) air at ambient temperature, they were able to obtain extensive data for flows at Reynolds numbers (based on the average speed and pipe diameter) much higher than in any previous experiment (from 31,000 up to 36×10^6). They divided the flow into several regions. In the near-wall, where $0 < y^+ < 60$, the flow is composed of the linear viscous sublayer and the buffer zone. Their detailed data followed by an asymptotic matching analysis suggested that two overlap regions appear in sufficiently high Reynolds number flows: a power-law region in the range $60 < y^+ < 500$ and a logarithm law in the range $600 < y^+ < 0.07K$ (here K is the Kármán number based on the friction speed and pipe radius). From their experimental data, they also demonstrated that the velocity deficit is the dominant outer (core region) velocity scale, which exhibits universality (independence of Reynolds number), whereas the friction speed is the dominant velocity scale near the wall. They also gave a modified friction factor relationship for a wide range of high Reynolds numbers.

Recently, McKeon et al. [11] performed additional experiments with Princeton's superpipe apparatus in the range of Re from 74,000 up to 36×10^6. They used smaller probe sizes for the measurement of the velocity and corrected the static pressure and mean velocity profiles. They confirmed the presence of the power-law region for $Re > 200,000$. They also found that the logarithmic law region holds for a larger range, $600 < y^+ < 0.12K$.

Another set of recent pipe flow experiments over a wide range of Reynolds numbers ($10 < Re < 1,000,000$) was conducted by

Received 10 December 2004; revision received 18 April 2006; accepted for publication 19 May 2006.

Swanson et al. [12] using the University of Oregon facility. A variety of gases, mostly at room temperature, was used to achieve both the laminar and the turbulent flow conditions and to experimentally determine the friction factor as function of Reynolds number for a fully developed pipe flow. These data were recently put together with the results from Princeton's superpipe experiments [7] and present the change of the friction factor in a fully developed pipe flows for the range of Re from 10 to 36 million (McKeon et al. [13]).

Wei et al. [14] have recently used detailed experimental data and direct numerical simulations of fully developed turbulent flows in free boundary layers, channels and pipes to propose a dynamically relevant four-layer description of the mean velocity profile. Each of the layers has been characterized by a predominance of two of the three terms in the Reynolds-averaged equation and its extent depends on the Reynolds number. They also claimed that the viscous effects may be important even at distances outside the buffer layer. A multiscale analysis was conducted to substantiate the four-layer structure. It verified the existence of an intermediate (meso) layer between the inner and outer layers where viscous and Reynolds stress gradients are in balance.

In this note, we use the Reynolds time-average equation for the mean axial speed, an extended form of Prandtl's mixing-length model for the turbulent stress, and a small subset of the available experimental data from McKeon et al. [11] to first estimate the mixing length as function of the distance from the walls scaled with the pipe radius, $\tilde{y}$. It is found that the nondimensional mixing-length curves are similar for all Reynolds numbers and may be represented by an average polynomial line, $\tilde{l}_{\text{ave}}(\tilde{y})$. This model line is also corrected by the van Driest [5] damping function. Then, to demonstrate the applicability of this new model curve, it is used in the Reynolds-averaged model equation to integrate the mean velocity profiles u^+ as function of $\tilde{y}$ from the wall to the pipe centerline at various Kármán numbers, K, and to compute the wall friction coefficient.

Extended Mixing-Length Concept

We consider a steady, incompressible, axially symmetric fully developed turbulent flow in a pipe of radius R with smooth walls. The pipe main axis is x and the vertical distance is $0 \le r \le R$ where $r = 0$ is the centerline and $r = R$ is the wall. The transverse mean speeds $v = w = 0$ and the mean axial speed $u(r)$ is described by the Reynolds-averaged equation [9]:

$$\frac{1}{r}\frac{\mathrm{d}}{\mathrm{d}r}\left[r\left(\mu\frac{\mathrm{d}u}{\mathrm{d}r} + (\sigma_{rx})_t\right)\right] = \frac{\mathrm{d}p}{\mathrm{d}x} \tag{1}$$

Here, μ is the fluid viscosity (assumed constant), $\mathrm{d}p/\mathrm{d}x$ is the constant axial gradient of the mean pressure, and $(\sigma_{rx})_t$is the Reynolds stress. The symmetry conditions at the centerline require that $(\mathrm{d}u/\mathrm{d}r)(0) = 0$ and $(\sigma_{rx})_t(0) = 0$. The no-slip condition at the pipe wall requires that $u(R) = 0$. It is also expected that there is no turbulent stress at the wall, $(\sigma_{rx})_t(R) = 0$.

Integrating (1) gives $\mu(\mathrm{d}u/\mathrm{d}r) + (\sigma_{rx})_t = (r/2)(\mathrm{d}p/\mathrm{d}x)$. Defining the friction velocity u_τ from the wall stresses by $\mu(\mathrm{d}u/\mathrm{d}r)(R) = (R/2)(\mathrm{d}p/\mathrm{d}x) = -\rho u_\tau^2$ (here ρ is the fluid constant density) gives

$$\mu\frac{\mathrm{d}u}{\mathrm{d}r} + (\sigma_{rx})_t = -\rho u_\tau^2\frac{r}{R} \tag{2}$$

Following Prandtl [3], we assume that the Reynolds stresses may be modeled by

$$(\sigma_{rx})_t = -\rho l^2\left|\frac{\mathrm{d}u}{\mathrm{d}r}\right|\frac{\mathrm{d}u}{\mathrm{d}r} \tag{3}$$

Here l is the mixing length. The negative sign in (3) is assumed because the expected speed gradients are negative in the entire range. Equations (2) and (3) can be used to compute the nondimensional mixing length (here $\nu = \mu/\rho$ is the kinematic viscosity):

$$\tilde{l} = \frac{l}{R} = \sqrt{\nu\frac{\mathrm{d}u}{\mathrm{d}r} + u_\tau^2\frac{r}{R}}\Big/\left(-\frac{\mathrm{d}u}{\mathrm{d}r}\right) \tag{4}$$

Using the data of McKeon et al. [11] for the measured velocity profiles at several (here, seven) Reynolds numbers ($Re = 2RU_{\text{ave}}/\nu$, where U_{ave} is the average axial speed) evenly distributed in the range between 74,300 and 35.7 million, and approximating the derivative $\mathrm{d}u/\mathrm{d}r$ by a second-order, nonuniform step, finite-difference formula, we computed for each Reynolds number the nondimensional mixing length as function of the nondimensional distance from the wall $\tilde{y} = 1 - r/R$. The computed results are shown in Fig. 1. The wavy nature of the computed points may be attributed to the error in computing the velocity derivative from the discretization of the experimental data. It can be seen that the nondimensional mixing-length curves are similar for all Reynolds numbers in the entire domain. The curves may be represented to the leading order by an average polynomial curve fit (independent of Reynolds number), in terms of the nondimensional distance from the wall:

$$\tilde{l}_{\text{ave}}(\tilde{y}) = 0.430\tilde{y} - 0.637\tilde{y}^2 + 0.577\tilde{y}^3 - 0.780\tilde{y}^4 + 0.660\tilde{y}^5 + \ldots \tag{5a}$$

for the range $0 < \tilde{y} < 0.9$. This curve is also shown in Fig. 1. It can be seen that near the wall the nondimensional average mixing length has a slope of about 0.43. This slope is close to the values of 0.42 found by McKeon et al. [11]. It should be noted that the largest global standard deviation of the individual curves from the average curve is 0.6% and the largest local absolute deviation is about 15% (for the lines at $Re = 74,300$ and $Re = 35.7$ million at $\tilde{y} \sim 0.65$).

It should be noted that the choice of seven Reynolds number cases is arbitrary. We find a very similar nondimensional mixing-length curve derived from any other set of the data, specifically when more cases are used. Moreover, we also computed the specific mixing-length curves for the cases where $Re = 74,300$ (lowest Reynolds number) and $Re = 35.7$ million (highest Reynolds number). It is found that the main difference between these lines and the line given by (5a) is around $\tilde{y} \sim 0.65$ where the local deviation is the largest, about 10%, and associated with the local scattering of the lines derived from the experimental data. Taking the average of these two lines gives a curve which is almost identical to the curve described by (5a). This demonstrates that the average nondimensional mixing-length curve can be deducted from only two cases of the data.

It should also be noted at this point that the experimental measurements are limited to certain distances from the wall and therefore do not allow an approximation of the nondimensional mixing length very near the wall, inside the viscous sublayer. The data from the experiments of Nikuradse [2], Zagarola and Smits [7],

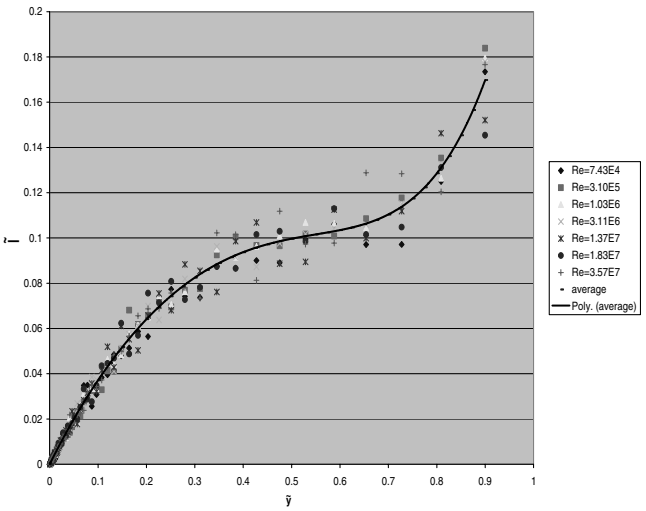

Fig. 1 Nondimensional mixing length as computed from data [11] and average curve (line).

and McKeon et al. [11] suggest that in the viscous sublayer the turbulent stresses are very small. Near the wall, we assume van Driest [5] damping function to correct the mixing-length formula.

$$\tilde{l} = \tilde{l}_{\text{ave}}(\tilde{y})\{1 - \exp(-y^+/A^+)\} \tag{5b}$$

Here $y^+ = u_\tau(R - r)/\nu$ is the classical nondimensional coordinate [3] in terms of distance from the wall and we find that $A^+ = 28$ provides the best fit with the experimental data of McKeon et al. [11]. When $y^+ > 3A^+$, the correction function is nearly 1 and there $\tilde{l} = \tilde{l}_{\text{ave}}(\tilde{y})$.

Analysis of Mean Velocity Profiles

To demonstrate the applicability of the proposed mixing-length curve according to (5a) and (5b), it is used now in Eqs. (2–4) instead of l. Let $u^+ = u/u_\tau$ be the nondimensional mean velocity. We find the following model equation

$$(\tilde{l})^2\left(\frac{\mathrm{d}u^+}{\mathrm{d}\tilde{y}}\right)^2 + \frac{1}{K}\left(\frac{\mathrm{d}u^+}{\mathrm{d}\tilde{y}}\right) - (1 - \tilde{y}) = 0 \tag{6}$$

with the wall condition $u^+(0; K) = 0$. Here K is the Kármán number defined as $K = Ru_\tau/\nu = \sqrt{[(-\mathrm{d}p/\mathrm{d}x)R^3]/2\rho\nu^2}$ for the pipe flow. Note that K is the only parameter in the problem (6) and it is determined by the pressure gradient, pipe radius, and flow properties. No additional empirical input is used to calculate the mean velocity. Also note that $\tilde{l} = \tilde{l}_{\text{ave}}(\tilde{y})\{1 - \exp(-K\tilde{y}/A^+)\}$. Equation (6) is written in a special way which accounts for the change of u^+ in terms of the global coordinate $\tilde{y}$ and not in terms of the near-wall coordinate y^+ as was written by Prandtl [3] (see also Pope [9]). Equation (6) gives

$$\frac{\mathrm{d}u^+}{\mathrm{d}\tilde{y}} = \frac{1}{(\tilde{l})^2}\left[-\frac{1}{2K} + \sqrt{\frac{1}{4K^2} + (\tilde{l})^2(1 - \tilde{y})}\right] \equiv g(\tilde{y}; K) \tag{7}$$

with the boundary (initial) condition $u^+(0; K) = 0$.

Equation (7) is integrated numerically from 0 to 1 for every value of K using a standard fourth-order Runge–Kutta integration scheme. Results for various values K of the computed mean velocity profiles are shown in Figs. 2a–2c. The blue (solid) lines represent the computed results and the red circles show the experimental data according to McKeon et al. [11]. All figures demonstrate a very nice agreement between the calculated mean velocities and the data for all values of K, including cases that were not used for the calculation of the universal mixing length. Moreover, we computed the mean velocities for all 28 cases reported by McKeon et al. [11] and found a very nice agreement with the experimental data for all cases (these are not shown in Figs. 2a–2c for clarity of the figures). Specifically, Fig. 2a describes the distribution of u^+in terms of the global coordinate $\tilde{y}$. The agreement between the results is remarkable.

Figure 2b describes the distribution of u^+ in terms of the near-wall coordinate $y^+ = K\tilde{y}$. This figure demonstrates from both the computations and data the universality (independence of K) of the pipe profile u^+as function of y^+ in the near-wall region. Similarly, Fig. 2c describes the scaled velocity deficit profiles $(U_{\max} - u)/(U_{\max} - U_{\text{ave}}) = (U^+_{\max} - u^+)/(U^+_{\max} - U^+_{\text{ave}})$ as function of the global coordinate $\tilde{y}$. Here, the parameter $U^+_{\text{ave}} \equiv U_{\text{ave}}/u_\tau = 2\int_0^1 u^+(\tilde{y}; K)(1 - \tilde{y})\,\mathrm{d}\tilde{y}$. The figure demonstrates from both the computations and data the universality (independence of K) of the pipe profiles $(U_{\max} - u)/(U_{\max} - U_{\text{ave}})$ as function of $\tilde{y}$ in the regions around the domain centerline for pipe flow case.

The resulting values of $Re = U^+_{\text{ave}}K$ as function of $K$are shown in Fig. 3. Except for the transition range $1,000 < Re < 4,000$ and $25 < K < 80$, the computed results exhibit a nice agreement with the experimental data for the range of Re from 10 to 36 million. When $K < 25$ (or $Re < 1,000$) the flow is laminar ($\tilde{y}_0 > 0.5$) and the classical relationship $Re = K^2/2$ holds whereas when the flow is turbulent ($Re > 4,000$) we find that $Re \sim 24K^{1.078}$.

Figure 4 describes the friction coefficient $f = 8(u_\tau/U_{\text{ave}})^2 = 8/(U^+_{\text{ave}})^2$ as function of the Reynolds number $Re = 2KU^+_{\text{ave}}$. The

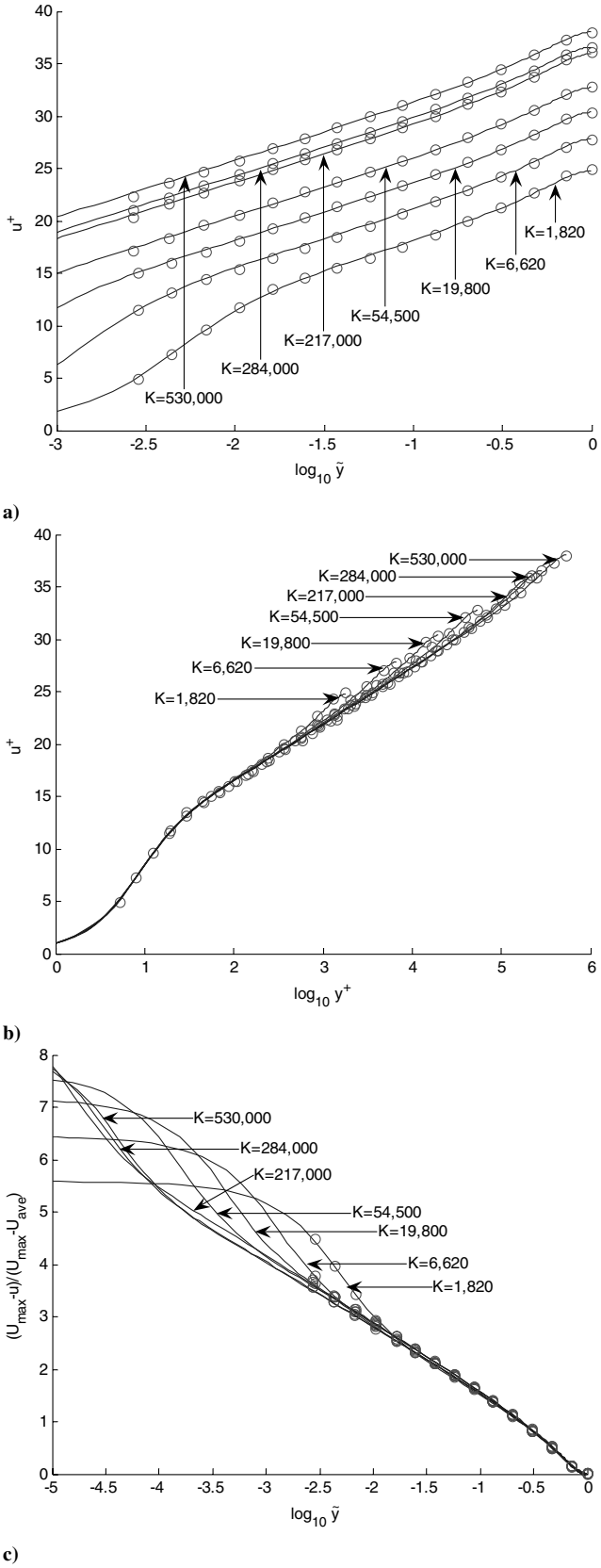

Fig. 2 Computed (lines) and measured (circles [11]) mean velocity profiles: a) u^+ vs $\log_{10}\tilde{y}$, b) u^+ vs $\log_{10}y^+$, c) $(U_{\max} - u)/(U_{\max} - U_{\text{ave}})$ vs $\log_{10}\tilde{y}$.

figure shows a nice agreement between the calculated values and the experimental results for the pipe flows from both the Princeton and Oregon facilities for all cases with Re between 5,000 and 36 million. Furthermore, we used the present model to compute the velocity profiles and friction factors for flow with $Re < 4,000$. The computed

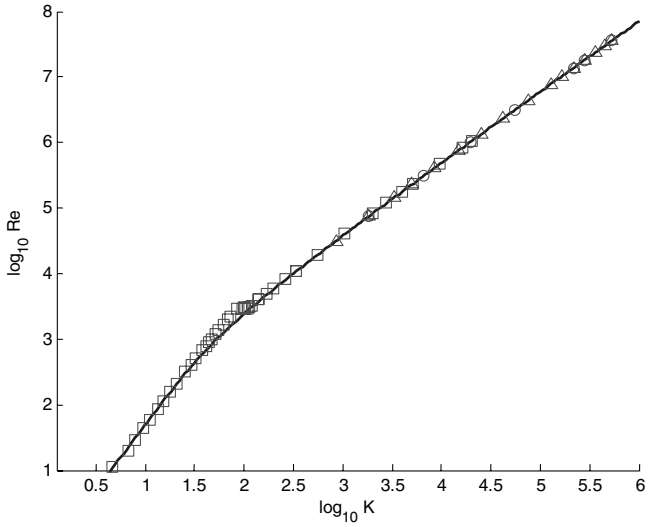

Fig. 3 Computed (line) and measured (squares, [12]; triangles, [7]; circles, [11]) *Re* vs *K*.

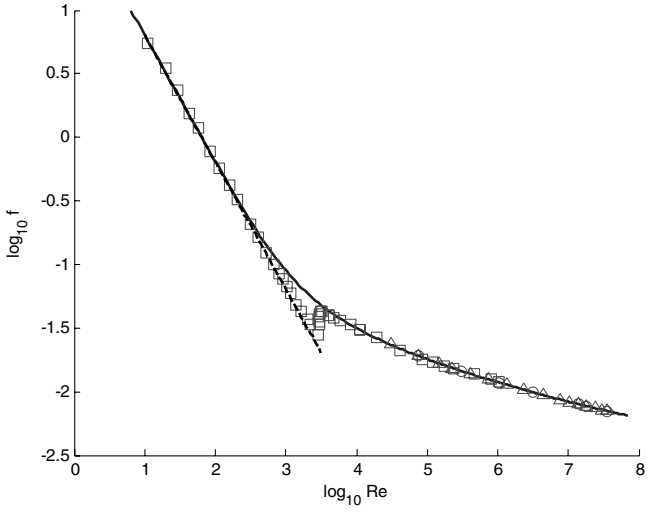

Fig. 4 Computed (solid line) and measured (squares, [13]; triangles, [7]; circles, [11]) f vs K; laminar flow result (dashed line).

results for f are also shown in Fig. 4. It can be seen that except for the transition region ($1,000 < Re < 4,000$ or $25 < K < 80$) the present predictions using Eq. (7) show a remarkable agreement with the available comprehensive experimental data for the range of Re between 10 and 36 million or K between 5 and 500,000. Here we used the relationship $K = \sqrt{f/32}Re$ to compute K for the experiments of Swanson et al. [12]. This demonstrates the validity of the present model from low to very high Reynolds number flows.

Discussion

For the pipe flow, it can be seen from the model Eq. (6) that the mean velocity u^+ is dominated by two different length scales, i.e.,

$$u^+ \approx u^+(1;K) + \int_1^{\tilde{y}} \frac{\sqrt{1-\tilde{y}'}}{\tilde{l}_{\text{ave}}(\tilde{y}')}\,\mathrm{d}\tilde{y}' + O\left(\frac{1}{K}\right) \quad \text{or}$$

$$\frac{u^+(1;K)-u^+}{u^+(1;K)-U^+_{\text{ave}}} \approx \frac{\int_{\tilde{y}}^1 g(\tilde{y}')\,\mathrm{d}\tilde{y}'}{\int_{\alpha/K}^1 \mathrm{d}\tilde{y}\int_{\tilde{y}}^1 g(\tilde{y}')\,\mathrm{d}\tilde{y}'} + O\left(\frac{1}{K}\right)$$

where $g(\tilde{y}') = \sqrt{1-\tilde{y}'}/\tilde{l}_{\text{ave}}(\tilde{y}')$ when $2\alpha/K \ll \tilde{y} \le 1$, whereas

$$u^+ \approx 12 + \int_{12}^{y^+} \frac{-1+\sqrt{1+4[0.445(y^+)']^2}}{2[0.445(y^+)']^2}\,\mathrm{d}(y^+)' + O\left(\frac{1}{K}\right)$$

when $12 \le y^+ \ll \alpha$ and $u^+ \approx y^+ + O\left(\frac{1}{K}\right)$ when $0 \le y^+ \le 12$

Here it is assumed that $\alpha \sim O(10^2)$. When the Kármán number is sufficiently high, these expansions explain the striking universality (independence of K) of the mean velocity profiles u^+ near the wall and of the velocity deficit profiles $(U^+_{\max} - u^+)/(U^+_{\max} - U^+_{\text{ave}})$ near the centerline.

Conclusions

The profiles of the mean velocities of fully developed turbulent flows in a pipe can be computed by the single model Eq. (7). The model uses the Reynolds-average equation for the mean axial speed, Prandtl's mixing-length model for the turbulent stress, and available experimental data from McKeon et al. [11] to establish that the nondimensional mixing-length curves may be represented to the leading order by the model line according to Eqs. (5a) and (5b). This curve is used in the model Eq. (7) to integrate the mean velocity profiles from the wall to the pipe centerline and compute the friction coefficient and Reynolds numbers at various Kármán numbers, K. The computed results of the velocity profiles show a remarkable agreement with the measured data. It is also demonstrated that the present model accurately predicts the friction factor according to both Oregon and Princeton's pipe facilities for a wide range of Re between 10 and 36 million, except for the transition region between 1,000 and 4,000. Moreover, the present analysis demonstrates the two main scales that govern the flow, $\tilde{y}$ and y^+, and the universality (independence of K) of the u^+ profiles near the wall and of the deficit velocity $(U_{\max} - u)/(U_{\max} - U_{\text{ave}})$ profiles as function of $\tilde{y}$ away from the wall and around the pipe centerline. We also demonstrate that the Kármán number is the only parameter that is needed to predict the mean velocity profile, the friction factor, and Reynolds number for any fully developed turbulent pipe flow.

References

[1] von Kármán, T., "Mechanishe Änlichkeit und Turbulenz," *Nachrichten von der Gesellschaft der Wissenschaften zu Gottingen, Mathematisch-Physikalische Klasse*, Germany, Jan. 1930, pp. 58–76 (English translation: *Proceedings of the Third International Congress on Applied Mechanics*, Stockholm, 1930, pp. 85–105).

[2] Nikuradse, J., "Gesetzmässigkeit der Turbulenten Strömung in Glatten Rohren," *Forschungsheft*, Vol. 356, Ausgabe B, Band 3, Sept.–Oct. 1932, pp. 1–36; English translation: "Laws of Turbulent Flow in Smooth Pipes," NASA TT-F-10359, Oct. 1966.

[3] Prandtl, L., "Recent Results of Turbulence Research," NACA TM 720, 1933.

[4] Millikan, C. M., "Critical Discussion of Turbulent Boundary Flows in Channels and Circular Tubes," *Proceedings of the 5th International Congress on Applied Mechanics*, Wiley, New York, 1938, 386–392.

[5] Van Driest, E. R., "On Turbulent Flow Near a Wall," *Journal of the Aerospace Sciences*, Vol. 23, Nov. 1956, pp. 1007–1011.

[6] Wosnik, M., Castillo, L., and George, W. K., "A Theory for Turbulent Pipe and Channel Flows," *Journal of Fluid Mechanics*, Vol. 421, Oct. 2000, pp. 115–145.

[7] Zagarola, M. V., and Smits, A. J., "Mean-Flow Scaling of Turbulent Pipe Flow," *Journal of Fluid Mechanics*, Vol. 373, Oct. 1998, pp. 33–79.

[8] Barenblatt, G. I., "Scaling Laws for Fully Developed Shear Flow. Part 1. Basic Hypotheses and Analysis," *Journal of Fluid Mechanics*, Vol. 248, March 1993, pp. 513–520.

[9] Pope, S. B., *Turbulent Flows*, Cambridge Univ. Press, Cambridge, England, U.K., 2000.

[10] George, W. K., and Castillo, L., "Zero-Pressure-Gradient Turbulent Boundary Layer," *Applied Mechanics Reviews*, Vol. 50, Dec. 1997, pp. 689–729.

[11] McKeon, B. J., Li, J., Jiang, W., Morrison, J. F., and Smits, A. J.,

"Further Observations on the Mean Velocity Distribution in Fully Developed Pipe Flow," *Journal of Fluid Mechanics*, Vol. 501, Feb. 2004, pp. 135–147 (see also http://gasdyn.princeton.edu/data/e248/mckeon_data.html [cited 10 Dec. 2004]).

[12] Swanson, C. J., Julian, B., Ihas, G. G., and Donnelly, R. J., "Pipe Flow Measurements over a Wide Range of Reynolds Numbers Using Liquid Helium and Various Gases," *Journal of Fluid Mechanics*, Vol. 461, June 2002, pp. 51–60.

[13] McKeon, B. J., Swanson, C. J., Zagarola, M. V., Donnelly, R. J., and Smits, A. J., "Friction Factors for Smooth Pipe Flow," *Journal of Fluid Mechanics*, Vol. 511, July 2004, pp. 41–44.

[14] Wei, T., Fife, P., Klewicki, J., and McMurtry, P., "Properties of the Mean Momentum Balance in Turbulent Boundary Layer, Pipe and Channel Flows," *Journal of Fluid Mechanics*, Vol. 522, Jan. 2004, pp. 303–327.

M. Sichel
Associate Editor